Applied Energy 167 (2016) 280–293

Contents lists available at ScienceDirect

Applied Energy

journal homepage: www.elsevier.com/locate/apenergy

# An NSGA-II based multi-objective optimization for combined gas and electricity network expansion planning ☆

Yuan Hu, Zhaohong Bie *, Tao Ding, Yanling Lin

*State Key Laboratory of Electrical Insulation and Power Equipment, Xi'an Jiaotong University, Xi'an 710049, China*

## HIGHLIGHTS

- Developed a multi-objective model for the combined natural gas network and electricity network.
- Taken into account the uncertainty and correlations of wind power in the proposed model.
- Presented an improved point-estimation method to solve the combined optimal power and natural gas load flow.

## ARTICLE INFO

*Article history:*
Received 30 June 2015
Received in revised form 21 October 2015
Accepted 22 October 2015
Available online 18 November 2015

*Keywords:*
Natural gas network expansion planning
Transmission expansion planning
Multi-objective
Primal–Dual Interior-Point method
Point-estimate method

## ABSTRACT

With the increasing proportion of natural gas in power generation, natural gas network and electricity network are closely coupled. Therefore, planning of any individual system regardless of such interdependence will increase the total cost of the whole combined systems. Therefore, a multi-objective optimization model for the combined gas and electricity network planning is presented in this work. To be specific, the objectives of the proposed model are to minimize both investment cost and production cost of the combined system while taking into account the $N-1$ network security criterion. Moreover, the stochastic nature of wind power generation is addressed in the proposed model. Consequently, it leads to a mixed integer non-linear, multi-objective, stochastic programming problem. To solve this complex model, the Elitist Non-dominated Sorting Genetic Algorithm II (NSGA-II) is employed to capture the optimal Pareto front, wherein the Primal–Dual Interior-Point (PDIP) method combined with the point-estimate method is adopted to evaluate the objective functions. In addition, decision makers can use a fuzzy decision making approach based on their preference to select the final optimal solution from the optimal Pareto front. The effectiveness of the proposed model and method are validated on a modified IEEE 24-bus electricity network integrated with a 15-node natural gas system as well as a real-world system of Hainan province.



## 1. Introduction

Driven by low prices and the increasingly stringent environmental regulations, natural gas accounts for 25% of the world's primary energy production at present. According to the recent projections, worldwide demand for natural gas is estimated to grow at a rate of 2.9–3.2% per year until 2030 [1]. By the end of the next decade, worldwide natural gas consumption is expected to be about 2.2 billion cubic meters (bcm) per day [2]. Owing to the distinct advantages of low cost, low carbon emission and fast response, gas-fired power generation keeps rising in the proportion of the total generating capacity in recent years, which leads to an increasing investment on the natural gas infrastructures. World Energy Outlook 2010 [3] shows that worldwide demand for natural gas in the power sector in 2008 was 4303 TW h, and it is projected to rise to 7600 TW h by 2035. In light of the observation results by the emission monitoring systems of United States, $CO_2$ emissions from U.S. power plants were 23% lower in 2012 than the emission amount in 1977 after replacing large number of fossil-fuel power plants by gas-fired plants [4]. Since the natural gas network is closely coupled with the electricity network by the gas-fired power plants, planning of any energy system regardless of such interdependence will increase the total cost of the entire combined energy

☆ This work was supported by the Doctoral Program of Higher Education for the Priority Development Areas (20130201130001), the Fundamental Research Funds for the Central Universities, and the Independence research project of State Key Laboratory of Electrical Insulation and Power Equipment in Xi'an Jiaotong University (EIPE14106).

* Corresponding author. Tel.: +86 29 8266 8655; fax: +86 29 8266 5489.
*E-mail address:* zhbie@mail.xjtu.edu.cn (Z. Bie).

http://dx.doi.org/10.1016/j.apenergy.2015.10.148
0306-2619/

**Nomenclature**

*Sets*

| | |
|---|---|
| $S_1$ | set of nodes in gas network |
| $SEP$ | set of existing pipelines |
| $SCP$ | set of candidate pipelines |
| $SEC$ | set of existing compressors |
| $SCC$ | set of candidate compressors |
| $SWS$ | set of gas supplier nodes |
| $SWL$ | set of gas load nodes |
| $S_2$ | set of nodes in electricity network |
| $SEL$ | set of existing transmission lines |
| $SCL$ | set of candidate transmission lines |
| $SG$ | set of generators |
| $SLoad$ | set of electricity demands |
| $\Gamma_1$ | set of gas-electricity combined nodes in gas network |
| $\Gamma_2$ | set of gas-electricity combined nodes in electricity network |
| $\Psi$ | set of normal operation and $N-1$ contingency states |

*Matrices*

| | |
|---|---|
| $A$ | pipe-nodal incidence matrix |
| $U$ | compressor node incidence matrix |
| $V$ | gas supplier-node incidence matrix |
| $C$ | gas load-node incidence matrix |
| $D$ | compressor fuel tap incidence matrix |
| $T$ | transmission line-node incidence matrix |
| $G$ | generator-node incidence matrix |
| $W$ | electricity load-node incidence matrix |

*Parameters*

| | |
|---|---|
| $NWS$ | number of gas suppliers |
| $NCG$ | number of coal-fired generators |
| $NGG$ | number of gas-fired generators |
| $NP$ | number of candidate pipelines and existing pipelines |
| $NC$ | number of candidate compressors and existing compressors |
| $NWL$ | number of gas loads |
| $NG$ | number of generators |
| $NL$ | number of transmission lines |
| $ND$ | number of electricity loads |
| $Cost_{gasi}$ | gas purchase cost of supplier $i$ |
| $CarbonCost$ | carbon emission price |
| $PlineCost_i$ | investment cost of installing pipeline $i$ |
| $ClineCost_i$ | investment cost of installing compressor $i$ |
| $ElineCost_i$ | investment cost of installing electricity line |
| $\varsigma$ | coefficient of converting net present value to annualized investment cost |
| $a_i, b_i, c_i$ | coefficients of the operation cost of generator $i$ |
| $\xi_1, \xi_2$ | carbon emission coefficient of coal-fired generator and gas-fired generator respectively |
| $\alpha_k, \beta_k, \gamma_k$ | gas consumption coefficients of compressor $k$ |
| $\mu_1, \mu_2, \mu_3$ | gas fuel rate coefficients of generator $i$ |
| $M_{ij}$ | gas pipeline constant depending on diameter, length, temperature, friction and gas composition |
| $\sigma_k$ | compressor constant depending on temperature, compressor efficiency and heat ratio |
| $Z_{ki}$ | gas compressibility factor at compressor inlet |
| $\delta$ | specific heat ratio |
| $R_k^{\max}$ | compression ratio of compressor $k$ |
| $WS_i^{\min}, WS_i^{\max}$ | max and min amount of gas supply at node $i$ |
| $\pi_i^{\min}, \pi_i^{\max}$ | max and min pressure at node $i$ |
| $B_k$ | electrical susceptance of transmission line $k$ |
| $\overline{F_k}$ | maximum capacity of transmission line $k$ |
| $P_{gk}^{\min}, P_{gk}^{\max}$ | max and min capacity of generator $k$ |
| $GHV$ | gas gross heating value |
| $PL_i^{\min}, PL_i^{\max}$ | max and min amount of load demand at node $i$ |
| $SM_{kc}$ | binary parameter that is 0 when the transmission line $k$is outage under state $c$ and, 1 otherwise |
| $WL_i$ | natural gas load at node $i$ |
| $PL_k$ | real power load at node $k$ |

*Variables*

| | |
|---|---|
| $x_i$ | binary decision variable, 1 if pipeline $i$ is installed, and 0 otherwise. |
| $y_i$ | binary decision variable, 1 if compressor $i$ is installed, and 0 otherwise |
| $z_i$ | binary decision variable, 1 if electricity line $i$ is installed, and 0 otherwise |
| $fP_k$ | natural gas flow of pipeline |
| $\pi_i, \pi_j$ | pressures at node$i$and, respectively |
| $WS_i$ | natural gas injection of gas supplier $i$ |
| $fc_k$ | gas flow rate at compressor $k$ |
| $H_k$ | power for compressor $k$ |
| $\tau_k$ | amount of gas tapped by compressor $k$ |
| $fl_k$ | power flow on transmission line $k$ |
| $\theta_{fr(k)}, \theta_{to(k)}$ | voltage angle at "from" and "to" buses of transmission line $k$ |
| $P_{gk}$ | real power supply from generator $k$ |
| $\Delta PL_i$ | amount of load curtailment at node $i$ |
| $fl_k^c$ | power flow on transmission line $k$ under state $c$ |
| $\theta_{fr(k)}^c, \theta_{to(k)}^c$ | voltage angle at "from" and "to" buses of transmission line $k$ under state $c$ |

systems. Therefore, it urgently calls for an effective planning method for the Combined Natural Gas Network and Electricity Network (CGEN) [5].

In the prior-at work, research that focuses on CGEN can be categorized into: (a) operation optimization and (b) expansion planning. Regarding the operation optimization of CGEN, the integrated optimal load flow problem for combined natural gas and electric power transmission networks has been analyzed in [6,7]. Specifically, in [6], a combined natural gas and electric optimal power flow is carried out to analyze the impact of the natural gas price variation on the optimal operation for CGEN; while in [7], an integrated load flow of CGEN has been presented considering the effect of temperature on the natural gas system operation. To improve the accuracy of the CGEN model, a multi-period CGEN optimization model has been developed in [8], where the natural gas storage, line-pack of pipeline, and power ramping characteristics of generators have been taken into account. In contrast, a mixed-integer linear program for the security-constrained optimal power and natural gas flow has been introduced in [9] to help system operators quickly respond to $N-1$ contingencies. Also, the natural gas network constraints are incorporated into the security-constrained unit commitment problem [10–12]. Compared to the CGEN operation optimization, CGEN expansion planning has become a hot research topic in recent years as many problems remain unsolved. Although [13] develops a long-term, multi-area and multi-stage planning model of CGEN, it only focuses on the system value chain as well as the optimal operation of existing

and new facilities, and most of the important elements of CGEN are simplified. In [5], a detailed CGEN optimization model is then proposed to achieve a low carbon integrated energy system, and the expansion decisions of the future CGEN, such as adding new natural gas pipes, compressors, and storage facilities of natural gas network and new transmission lines of electricity network, can be determined. Ref. [14] presents a multi-period integrated framework for generation, transmission and natural gas network expansion planning, but the modeling of compressor is neglected and the new method to solve natural gas load flow is only applicable to radical natural gas networks. Considering the uncertainties brought by an increasing utilization of natural gas in the power system, Ref. [15] presents an integrated expansion planning framework for CGEN with the aim to maximize the benefit–cost ratio by evaluating benefits in operation reduction, carbon emission reduction and reliability improvement against the increase in investment costs.

In recent years, wind energy is one of the rapidly growing renewable energies [16]. Unlike the traditional controllable power energy supplied by fossil fuel-based power plants, generation by wind energy is volatile due to the fluctuation of wind speeds, which brings about a great challenge to the operation and planning in power systems [17]. On the other hand, the natural gas network is closely coupled with the electricity network, which should be relevant to implement the research of CGEN expansion planning taking into account the uncertainty of wind power. Ref. [18] develops a CGEN model to investigate the impact of a large amount of wind energy on the British natural gas network. The results show that gas-fired generation can be used to compensate the wind energy variability, and the natural gas storage facilities as well as gas-fired plants with dual-fuel capability are suggested to mitigate the variability of wind energy. Ref. [19] proposes a robust optimization approach to analyze the interdependency among natural gas, coal and electricity infrastructures considering their operation constraints and wind energy uncertainties. However, there are few papers addressing CGEN expansion planning with the consideration of wind energy uncertainties.

For transmission network expansion planning, it is very important to take into account the "$N-1$" network security criterion [20]. The conventional process of conducting "$N-1$" network security criteria is that firstly optimizing a scheme without accounting for any component failure, and then checking the "$N-1$" security for the obtained scheme. If it is not satisfied, expanding the scheme further until the "$N-1$" deterministic security criterion is met [21].

In light of the above issues, this paper presents a multi-objective optimization model for the CGEN expansion planning considering uncertain wind power generation as well as the "$N-1$" network security criterion. The objective of the proposed model is to minimize the total investment cost and production cost by expanding appropriate pipelines, compressors and electricity lines, while satisfying the future load growth and additional security and operational constraints. In fact, the proposed model is a multi-objective, mixed integer non-linear stochastic problem, which cannot be easily solved by classical mathematical techniques. In this paper, the Elitist Non-dominated Sorting Genetic Algorithm II (NSGA-II) [22] is applied to the proposed model, and the Primal–Dual Interior-Point (PDIP) method combined with the point-estimation method is adopted to evaluate the objective functions and capture the final optimal Pareto front. Finally, decision makers can use a fuzzy decision-making approach based on their preference to select the final optimal solution from the optimal Pareto front.

The main contributions of this paper are suggested as follows:

(1) A multi-objective model is developed to simultaneously minimize the investment cost and production cost of the CGEN. Most importantly, the $N-1$ electricity network security criterion is considered in the optimization process.
(2) The primal–dual interior-point method combined with the improved point-estimation method is proposed to solve the combined optimal power and natural gas load flow.
(3) The NSGA-II method is deployed to capture the Pareto front of the proposed multi-objective model and furthermore, the final planning scheme can be selected based on the preference of decision-maker.

The rest of the paper is organized as follows. Section 2 presents the mathematical formulation of the multi-objective CGEN model considering wind power uncertainties. Section 3 shows the NSGA-II method for capturing the Pareto set of proposed model. The numerical results are presented in Section 4, where the impact of wind power uncertainties on the CGEN planning scheme is also discussed. Finally, conclusions are drawn in Section 5.

## 2. Mathematical formulation of the CGEN expansion planning model

### 2.1. Deterministic CGEN expansion planning model

A natural gas network includes gas producers, pipelines, gas compressors, interconnection points, storage facilities and gas consumers. In this paper, only three basic types of entities, pipelines, compressor stations and interconnection points are considered for the modeling of natural gas network. It is assumed that all the compressors are driven by gas energy, and the natural gas is tapped from the inlet node of each compressor. The electricity network is represented by a DC power flow model, so the reactive power and voltage amplitude are neglected. Natural gas network and electricity network are closely linked by gas-fired generators, which can be treated as energy converters between these two energy systems. To natural gas network, gas-fired generators are treated as natural gas loads, while for electricity network they are considered as power supplies.

As the natural gas load and electricity load increase in the planning horizon year, the objective of the proposed model is to determine *which* and *where* candidate pipelines, compressors and electricity lines should be constructed to achieve the minimum investment cost while satisfying the future energy requirement. Certainly, transmission structures have great impacts on the optimal operation for both natural gas network and electricity network and we also expect to minimize the production cost of natural gas supply and power generation. Meanwhile, to achieve the low-carbon economy, the carbon emission cost of power generation is also considered as a part of the production cost. In addition, the operation and security constraints of CGEN should be strictly considered, so the mathematical formulation of the proposed co-planning model can be expressed as follows:

$$Min\ f_1 = InvestmentCost$$

$$InvestmentCost = \varsigma \cdot \left( \sum_{i=1}^{NCP} x_i PlineCost_i + \sum_{i=1}^{NCC} y_i ClineCost_i + \sum_{i=1}^{NCL} z_i ElineCost_i \right) \quad (1)$$

$$Min\ f_2 = ProductionCost + CarbonEmissionCost$$

$$ProductionCost = \sum_{i=1}^{NWS} 8760 \cdot Cost_{gasi} * WS_i + 8760 \cdot \sum_{i=1}^{NCG} (a_i P_{gi}^2 + b_i P_{gi} + c_i) \quad (2)$$

$$CarbonEmissionCost = \sum_{i=1}^{NCG} 8760 \cdot CarbonCost * \xi_1 * P_{gi} + \sum_{i=1}^{NGG} 8760 \cdot CarbonCost * \xi_2 * P_{gi} \quad (3)$$

Subject to:

(1) Natural gas network constraints

Gas pipeline constraints

$$fP_k^2 = \mathrm{sgn}_{ij} M_{ij} \left(\pi_i^2 - \pi_j^2\right) \qquad k \in SEP, \quad i,j \in S_1 \quad (4)$$

$$-\overline{fP_k} \leqslant fP_k \leqslant \overline{fP_k} \qquad k \in SEP, \quad i,j \in S_1 \quad (5)$$

$$sgn_{ij} = \begin{cases} +1 & \pi_i > \pi_j \\ -1 & \pi_i < \pi_j \end{cases} \quad (6)$$

$$-M_1(1-z_k) \leqslant fP_k^2 - \mathrm{sgn}_{ij} M_{ij}(\pi_i^2 - \pi_j^2) \leqslant M_1(1-z_k) \qquad k \in SCP, \ \forall i,j \in S_1 \quad (7)$$

$$-z_k \overline{fP_k} \leqslant fP_k \leqslant z_k \overline{fP_k} \qquad k \in SCP, \quad \forall i,j \in S_1 \quad (8)$$

Compressor operation constraints

$$H_k = \sigma_k fc_k \left[ \left( \frac{\pi_j}{\pi_i} \right)^{Z_{ki}\left(\frac{\delta-1}{\delta}\right)} - 1 \right] \qquad k \in SEC \bigcup SCC, \quad i,j \in S_1 \quad (9)$$

$$\tau_k = \gamma_k H_k^2 + \beta_k H_k + \alpha_k \quad k \in SEC \bigcup SCC \quad (10)$$

$$1 \leqslant \frac{\pi_j}{\pi_i} \leqslant R_k^{\max} \qquad k \in SEC \bigcup SCC, \quad i,j \in S_1 \quad (11)$$

$$0 \leqslant \frac{\pi_j}{\pi_i} - 1 \leqslant y_k R_k^{\max} \qquad k \in SCC, \quad i,j \in S_1 \quad (12)$$

Nodal pressure constraints

$$\pi_i^{\min} \leqslant \pi_i \leqslant \pi_i^{\min} \quad \forall i \in S_1 \quad (13)$$

Natural gas supply constraints

$$WS_i^{\min} \leqslant WS_i \leqslant WS_i^{\max} \quad \forall i \in SWS \quad (14)$$

Nodal natural gas flow balance equation

$$\sum_{i=1}^{NP} A_{mi} \cdot fp_i + \sum_{i=1}^{NC} U_{mi} \cdot fc_i + \sum_{i=1}^{NWS} V_{mi} WS_i - \sum_{i=1}^{NWL} C_{mi} WL_i - \sum_{i=1}^{NC} D_{mi} \tau_i = 0 \quad \forall m \in N_1 \quad (15)$$

(2) Electricity network constraints

Electricity line power flow constraints

$$fl_k = B_k(\theta_{fr(k)} - \theta_{to(k)}) \qquad \forall k \in SEL \quad \theta_{fr(k)}, \theta_{to(k)} \in S_2 \quad (16)$$

$$-\overline{F_k} \leqslant fl_k \leqslant \overline{F_k} \quad \forall k \in SEL \quad (17)$$

$$-M_k(1-z_k) \leqslant fl_k - B_k(\theta_{fr(k)} - \theta_{to(k)}) \leqslant M_k(1-z_k) \quad \forall k \in SCL \quad (18)$$

$$-z_k \overline{F_k} \leqslant fl_k \leqslant z_k \overline{F_k} \quad \forall k \in SCL \quad (19)$$

Generation constraints

$$P_{gk}^{\min} \leqslant P_{gk} \leqslant P_{gk}^{\max} \quad \forall k \in SG \quad (20)$$

Node balance constraints for electricity network

$$\sum_{i=1}^{NL} T_{mi} fl_i + \sum_{i=1}^{NG} G_{mi} P_{gi} - \sum_{i=1}^{ND} W_{mi} PL_i = 0 \quad \forall m \in S_2 \quad (21)$$

(3) Equality constraints for joint gas and electricity

$$WL_k = \left(\mu_1 P_{gi}^2 + \mu_2 P_{gi} + \mu_3\right) \Big/ GHV \qquad k \in \Gamma_1, \quad i \in \Gamma_2 \quad (22)$$

The first objective is the investment costs of selected gas pipelines, compressors and electricity lines. The second objective function is to minimize the production cost including the carbon emission cost under constraints (4)–(22). The production cost and carbon emission cost are represented by Eqs. (2) and (3), respectively. It should be noted that the production cost and the carbon emission cost of coal-fired generators and gas-fired generators are calculated separately.

The constraints of the proposed CGEN optimization model include three parts: (a) constraints (4)–(15) represent the operation and security constraints of natural gas network; (b) constraints (16)–(21) refer to the operation and security constraints of electricity network; and (c) constraint (22) is the energy conversion equality constraint which links the two systems together. To be specific, constraints (4)–(6) represent the operation constrains of existing gas pipelines, and constraints (7) and (8) represent the operation constrains of candidate gas pipelines, where $M_1$, often called "big M" value, represents a large enough input value. This parameter is applied to guarantee the constraint (7) to be inactive if the pipeline $k$ is not selected. The appropriate value of $M_1$ can be referred to [1]. Constraints (9)–(11) represent the operation constrains of both existing and candidate gas compressors. When the candidate compressor is not selected, the pressure at the inlet node of compressor will be equal to the pressure at outlet node by the constraint (12), and then we can treat the compressor as an interconnection point. Constraints (18) and (19) represent the operation and security constraints of candidate transmission lines, respectively. The effect of Parameter $M_k$ is the same as that of $M_1$, and we set it as $1.2B_k$ in this paper. The detailed discussion on setting a proper value for $M_k$ can be referred to [23].

### 2.2. Deterministic CGEN expansion planning model considering N−1 network security criterion

Assuming that the stored natural gas can be used to avoid natural gas load curtailment if a contingency occurs in the natural gas network, we thus only consider the $N-1$ network security criterion for the electricity network. It should be noted that the outage of the generator is neglected in this paper, so the number of $N-1$ electricity line contingency states is $N$. First of all, an $NL \times (NL+1)$ state matrix $SM$ is introduced to represent the normal operation and $N-1$ contingency states, in which the row number equals to the number of electricity lines and the column number equals to the number of normal operation state plus $N-1$ contingency states, yielding

$$SM = \begin{bmatrix} 1 & 0 & 1 & \cdots & 1 \\ 1 & 1 & 0 & \cdots & 1 \\ \vdots & \vdots & \vdots & \cdots & \vdots \\ \vdots & \vdots & \vdots & \cdots & \vdots \\ \vdots & \vdots & \vdots & \cdots & \vdots \\ 1 & 1 & 1 & \cdots & 0 \end{bmatrix}_{NL \times (NL+1)} \quad (23)$$

The first column of matrix $SM$ represents the normal operation states, and all the element values are 1 indicating all electricity lines can operate normally. The other columns of the matrix $SM$represent $N-1$ electricity line contingency states, and each column only has one element with value set as 0 to represent that this electricity is outage. Then, a mixed integer linear programming model with minimizing total load curtailment of electricity network under normal and $N-1$ contingency states can be written as:

$$Min\ LoadSheddingAmount = \sum_{i=1}^{ND} \Delta PL_i \tag{24}$$

Subject to

$$\begin{aligned} -M_k(1 - SM_{kc}) &\leqslant fl_k^c - B_k\left(\theta_{fr(k)}^c - \theta_{to(k)}^c\right) \\ &\leqslant M_k(1 - SM_{kc}) \quad \forall k \in SEL \quad fr(k),\ \mathrm{to}(k) \\ &\in S_2 c \in \Psi \end{aligned} \tag{25}$$

$$-SM_{kc}\overline{F_k} \leqslant fl_k^c \leqslant SM_{kc}\overline{F_k} \quad \forall k \in SEL\ c \in \Psi \tag{26}$$

$$\begin{aligned} -M_k(2 - z_k - SM_{kc}) &\leqslant fl_k^c - B_k\left(\theta_{fr(k)}^c - \theta_{to(k)}^c\right) \\ &\leqslant M_k(2 - z_k - SM_{kc}) \\ &\forall k \in SCL \quad fr(k),\ \mathrm{to}(k) \in S_2\ c \in \Psi \end{aligned} \tag{27}$$

$$-z_k SM_{kc}\overline{F_k} \leqslant fl_k \leqslant z_k SM_{kc}\overline{F_k} \quad \forall k \in SCL \quad c \in \Psi \tag{28}$$

$$PL_i^{\min} \leqslant \Delta PL_i \leqslant PL_i^{\max} \quad \forall i \in SLoad \tag{29}$$

$$\sum_{i=1}^{NL} T_{mi} fl_i + \sum_{i=1}^{NG} G_{mi} P_{gi} + \sum_{i=1}^{ND} W_{mi} \Delta PL_i - \sum_{i=1}^{ND} W_{mi} PL_i = 0 \quad \forall m \in S_2 \tag{30}$$

Gas network constraints (4)–(15).

Electricity network constraints (20).

Gas and electric combined node equality constraints (22).

In the above formulation, constraints (25)–(28) represent the operation and security constraints of candidate electricity lines under normal and $N-1$ contingency states. Constraints (25) and (26) will become inactive if the value of $SM_{kc}$ is 0, and 1 otherwise. Constraints (27) and (28) only become active when the values of $z_k$ and $SM_{kc}$ are set as 1 simultaneously, which means that the electricity line $k$ is selected and it can normally operate. In other situations, both constraints (27) and (28) are inactive constraints.

To guarantee the final scheme satisfy the $N-1$ network security criterion for the electricity network, we treat the amount of load curtailment as a penalty term and add it to the first two objectives. Then the new objectives are as follows:

$$Min\ f_1 = InvestmentCost + Penalty_1 \cdot LoadSheddingAmount \tag{31}$$

$$\begin{aligned} Min\ f_2 = {} & ProductionCost + CarbonEmissionCost + Penalty_2 \\ & \cdot LoadSheddingAmount \end{aligned} \tag{32}$$

where $Penalty_1$ and $Penalty_2$ are the coefficients of penalty term, and both of them are set as 1000.

### 2.3. Stochastic CGEN expansion planning model considering N−1 network security criterion

The wind energy is intermittent and uncertain, so the value of the second objective becomes a stochastic variable. Taking into account the uncertain wind energy, we establish a multi-objective stochastic model for the CGEN expansion planning with the investment cost and the expected production cost, carbon emission cost and the amount of load curtailment as objectives. The mathematical formulation is as follows

$$Min\ f_1 = InvestmentCost + Penalty_1 \cdot \mu_{LoadSheddingAmount} \tag{33}$$

$$Min\ f_2 = \mu_{PECost} + Penalty_2 \cdot \mu_{LoadSheddingAmount} \tag{34}$$

$$\mu_{LoadSheddingAmount} = E\left(\sum_{i=1}^{ND} \Delta PL_i\right) \tag{35}$$

Subject to constraints (4)–(15), (20), (22), (26)–(30).

$$\begin{aligned} \mu_{PECost} = E\Bigg(& \sum_{i=1}^{NWS} 8760 \cdot Cost_{gasi} * WS_i + 8760 \cdot \sum_{i=1}^{NCG}\left(a_i P_{gi}^2 + b_i P_{gi} + c_i\right) \\ & + \sum_{i=1}^{NCG} 8760 \cdot CarbonCost * \xi_1 * P_{gi} + \sum_{i=1}^{NGG} 8760 \cdot CarbonCost \\ & * \xi_2 * P_{gi}\Bigg) \end{aligned} \tag{36}$$

Subject to constraints (4)–(22).

In order to remove the binary variable $sgn_{ij}$ in Eq. (6) and make this model solvable by the optimization tool IPOPT, we introduce two new continuous variables $s_k$ and $t_k$ , and make the following transformation for constraints (4) and (6).

$$fP_k = (1 - 2s_k) \cdot t_k \tag{37}$$

$$t_k^4 = M_{ij}^2\left(\pi_i^2 - \pi_j^2\right)^2 \tag{38}$$

$$-Ms_k <= \pi_i - \pi_j <= M(1 - s_k) \tag{39}$$

$$s_k(1 - s_k) = 0 \tag{40}$$

where $M$ is a large value, and we set it as 10,000 in this paper. Then, all the proposed models only include three binary decision variables for candidate pipelines, compressors and electricity lines. This transformation will facilitate the proposed algorithm introduced in the next section.

## 3. NSGA-II based multi-objective optimization model

In the traditional network expansion planning study, the natural gas network and electricity network are implemented independently. For each of them, the optimization model is a mixed integer non-linear programming problem (MINLP). However, when these two models are combined together by a series of nonlinear energy conversion equation constraints, it becomes a CGEN co-planning model which is complex and difficult to solve. To address this problem, we employ a heuristic algorithm "Elitist Non-dominated Sorting Genetic Algorithm" (NSGA II) [22] combined with the IPOPT (Interior Point Optimizer) to solve the proposed model.

It should be noted that the integer decision variables of the proposed model including three parts: candidate pipelines, candidate compressors and candidate electricity lines, and the decimal coding is adopted in the proposed algorithm. Based on the NSGA-II for multi-objective optimization problem, the whole procedure for solving the proposed model, which is shown in Fig. 1, can be summarized as follows:

*Step 1*: Set iteration counter $t = 0$, a population $P(t)$ with predefined size randomly generated, in which each individual represents a scheme to add candidate pipelines, compressors and electricity lines on the base CGEN.

*Step 2*: The objective functions of each scheme can be evaluated as shown in the red box of Fig. 1, and then according to

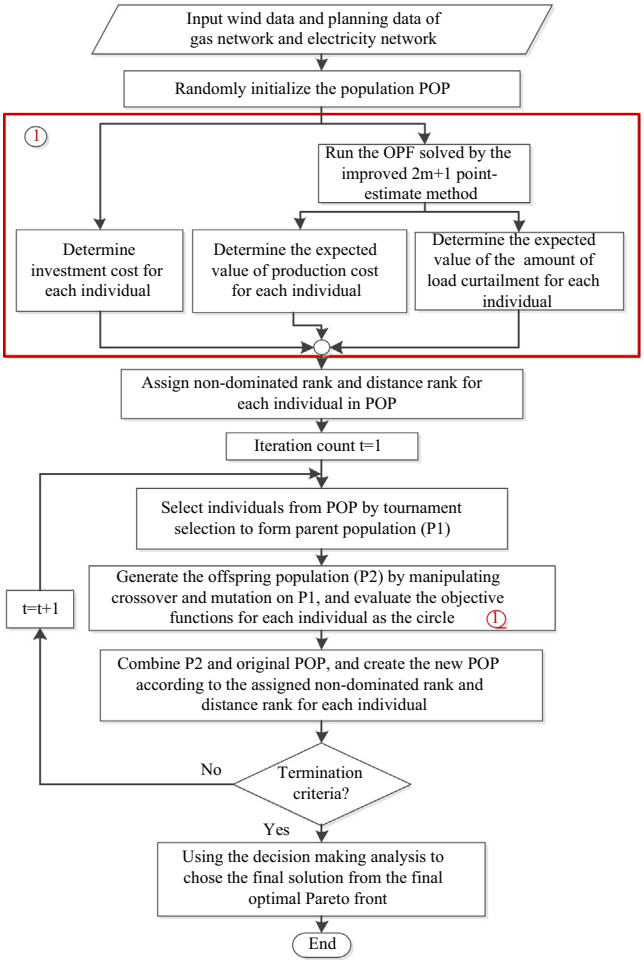


**Fig. 1.** Flowchart of the proposed algorithm.

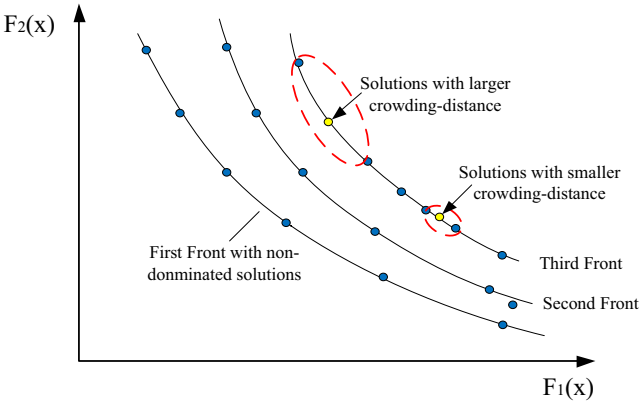


**Fig. 2.** Population classified by non-dominated sorting technique.

non-domination ranks and crowding-distance values, all schemes are classified into a number of non-dominated fronts as shown in Fig. 2. The detailed process to achieve objective functions of each scheme will be introduced in the section 3.1.

*Step 3*: Apply a binary tournament selection on $P(t)$ to form the parent population $S(t)$, where schemes with lower non-domination rank or larger crowding distance value, as presented in Fig. 2, have more chance to be selected.

*Step 4*: Manipulate crossover and mutation operators on parent population $S(t)$, so new schemes can be reproduced to create offspring population $Q(t)$. And then calculate objective functions for each scheme in $Q(t)$.

*Step 5*: Combine population $P(t)$ with population $Q(t)$ to develop $R(t)$, and carry out non-dominated sorting on $R(t)$, then a new population $P(t)$ is generated from $R(t)$. The detailed forming process is shown in Fig. 3. It can be seen that the schemes, belonging to the lower front or with larger crowding-distance, have a higher priority of being selected for reproduction. Therefore, candidate gas pipelines, gas compressor and transmission lines with larger contribution to attain desirable objective functions are selected.

*Step 6*: Set $t = t + 1$, and verify whether the value of iteration count reaches the maximum number of predefined iterations. If it is not satisfied, go back to Step 3; otherwise, stop the iterative search and output the optimal Pareto front of the planning schemes.

*Step 7*: To obtain the final planning scheme from the optimal Pareto front, a fuzzy satisfying method is adopted to help the planner make the final decision.

However, there are two issues that should be addressed in section 3.1 and 3.2.

### 3.1. Evaluation of objective functions

Because the value of candidate pipelines, compressors and electricity lines is known for each scheme, the first objective (investment cost) of each scheme in population can be easily obtained. Meanwhile, when solving the second objective, the original MINLP model becomes a non-linear programming problem which can be solved by the IPOPT solver. So the difficult problem is how to tackle the uncertainty and correlations of wind power.

An improved Point Estimate Method (PEM) proposed in [24] is extended to calculate the expected value of second objective (production cost and amount of load curtailment). Comparing to the traditional commonly used methods, such as the Monte Carlo Simulation, the employed method can significantly reduce the computational time especially for large-scale optimization model. Assuming that there are m wind farms, the approximation of expected value of second objective can be obtained only by calculating $2m + 1$ times deterministic optimal power and natural gas load flow via IPOPT.

Unlike PEM that requires uncorrelated random variables, the improved PEM can take the effects of the correlations among wind farm outputs into consideration, by using an orthogonal transformation. Therefore, the correlated input variables are converted into variables with independent distribution, and the traditional PEM can be deployed.

The improved PEM method to calculate the expected value of second objective is divided into two stages. The first stage is to achieve correlated outputs of wind farms as input data, and the second stage is applying this input data to evaluate the expected objective value.

#### 3.1.1. Obtaining correlated wind farm output

In this paper, the commonly used Weibull distribution [25] is chosen to simulate the volatile wind speed, and the correlations among wind speeds of different wind farms can be represented by a correlation matrix [24] as:

$$C_W = (\rho_{ij}) = \begin{pmatrix} \rho_{11} & \rho_{12} & \cdots & \rho_{1n} \\ \rho_{21} & \rho_{22} & \cdots & \rho_{2n} \\ \vdots & \vdots & \cdots & \vdots \\ \rho_{n1} & \rho_{n2} & \cdots & \rho_{nn} \end{pmatrix} \tag{41}$$

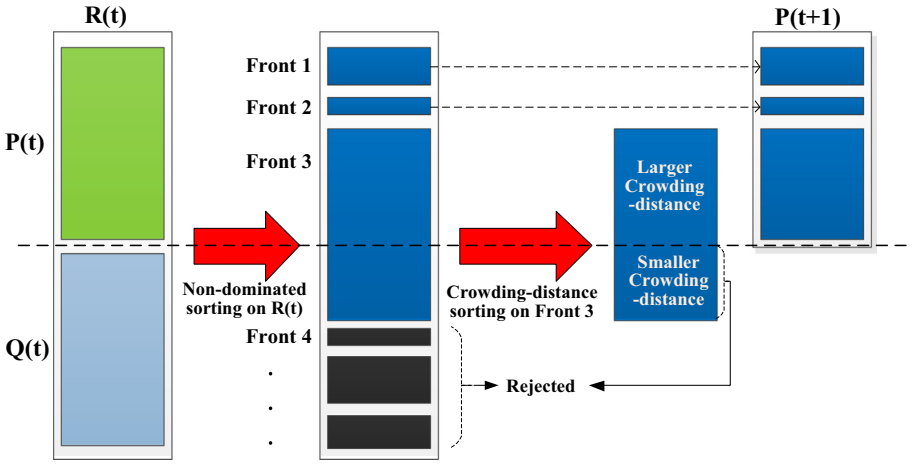


**Fig. 3.** Forming process of new population.

where $\rho_{ij}$ is the correlation coefficient between wind speed variable $V_i$ and wind speed variable $V_j$.

Given the Weibull distribution parameters and the correlation matrix of wind speeds, the method of generating the correlated wind speeds can be referred to [26]. And then the correlated outputs of wind farms can be obtained by Eq. (42).

$$P_w = \begin{cases} 0 & V < V_{ci}, \quad V > V_{co} \\ P_{rate}(V - V_{ci})/(V_{rate} - V_{ci}) & V_{ci} \leqslant V < V_{rate} \\ P_{rate} & V_{rate} \leqslant V \leqslant V_{co} \end{cases} \tag{42}$$

where $P_{rate}$ is the rated power of wind turbine, $V_{ci}, V_{rate}$ and $V_{co}$ are the cut-in, rated, cut-out wind speed, respectively. After obtaining a large number of simulated wind power data, the first four statistical moments of each wind farm can be easily calculated by mathematical statistics analysis method [26]. Meanwhile, the variance–covariance matrix, which represents the correlations among the wind power outputs, can also be easily obtained from correlation matrix $C_W$.

Certainly, if enough data of measured weed speed is known to planner, it can be directly applied to calculate the first four statistical moments and variance–covariance matrix as input data of wind farms.

### 3.1.2. Evaluating the second objective by the Improved PEM

Let vector $X$ represent the correlated output of $m$ wind farms and $Y$ be the second objective function, and the detailed procedure of applying the improved PEM is summarized as follows to evaluate the expected objective value:

(1) Input the first four statistical moments of the $m$ wind farms outputs, including column vectors of the means $\mu_X$, standard deviations $\delta_X$, skewness $\lambda_{X,3}$ and kurtosis $\lambda_{X,4}$, as well as the variance–covariance matrix $C_X$.
(2) Obtain inferior triangular matrix $L$ by decomposing $C_X$ through Cholesky decomposition, $C_X = LL^T$.
(3) Calculate the first four central moments of vector $Z$ with independent variables (corresponding to correlated vector $X$ ) as follows:

$$\mu_Z = L^{-1}\mu_X \tag{43}$$

$$C_Z = L^{-1}C_X(L^{-1})^T = I \tag{44}$$

$$\lambda_{Zl,3} = \sum_{r=1}^{m}\left(L_{lr}^{-1}\right)^3 \lambda_{Xr,3}\delta_{Xr} \quad l = 1,\ldots m \tag{45}$$

$$\lambda_{Zl,4} = \sum_{r=1}^{m}\left(L_{lr}^{-1}\right)^4 \lambda_{Xr,4}\delta_{Xr} \quad l = 1,\ldots m \tag{46}$$

(4) Calculate the concentrations $((z_{l,k}, \omega_{l,k}), k = 1,2,3$ $l = 1,\ldots m)$ in the transformed independent space according to Eqs. (47)–(51).

$$\xi_{l,k} = \frac{\lambda_{Zl,3}}{2} + (-1)^{3-k}\sqrt{\lambda_{Zl,4} - \frac{3}{4}\lambda_{Zl,3}^2}, \quad k = 1,2 \tag{47}$$

$$\xi_{l,3} = 0 \tag{48}$$

$$\omega_{l,k} = \frac{(-1)^{3-k}}{\xi_{l,k}(\xi_{l,1} - \xi_{l,2})}, \quad k = 1,2 \tag{49}$$

$$\omega_{l,3} = \frac{1}{m} - \frac{1}{\lambda_{Zl,4} - \lambda_{Zl,3}^2} \tag{50}$$

$$z_{l,k} = \mu_{Zl} + \xi_{l,k}\cdot\delta_{Zl}, \quad k = 1,2 \tag{51}$$

(5) Construct the $3m$ transformed points in the form $(Z_l^k = (\mu_{Z1}, \mu_{Z2}, \ldots z_{l,k}, \ldots, \mu_{Zm})\ k = 1,2,3 l = 1,\ldots m)$, and convert these points into the original space by applying the inverse transformation, that is, $X_l^k = LZ_l^k,\ k = 1,2,3 \quad l = 1,\ldots m$.
(6) Solve $3m$ times deterministic optimal power and natural gas load flow $(Y_l^k = H(X_l^k)\ k = 1,2,3\ l = 1,\ldots m)$, and then the expected value of $Y$ can be obtained as follows:

$$\mu_Y \cong \sum_{l=1}^{m}\sum_{k=1}^{3}\omega_{l,k} \times H(X_l^k) \tag{52}$$

It should be noted that m of 3 m points are at the same point $(\mu_{X1}, \mu_{X2}, \ldots \mu_{Xk}, \ldots, \mu_{Xm})$, so in fact only $2m + 1$ iterations are need to yield the approximation of the expected value of $Y$.

## 3.2. Final deterministic decision-making

Obviously, the result of multi-objective optimization problems should be a Pareto set. To obtain the final planning scheme, a fuzzy satisfying method using the distance metric method is adopted to help the planner make the final decision [27].

Firstly, map all the schemes in the final optimal Pareto front into fuzzy sets. The fuzzy sets are defined by a linear membership function as follows:

$$\mu_{f_i}(x)=\begin{cases}0 & f_i(x)>f_i^{\max}\\ \frac{f_i^{\max}-f_i(x)}{f_i^{\max}-f_i^{\min}} & f_i^{\min}\leqslant f_i(x)\leqslant f_i^{\max}\\ 1 & f_i(x)<f_i^{\min}\end{cases} \tag{53}$$

where $f_i^{\max}$ and $f_i^{\min}$ denote the maximum and minimum value of objective function $i$ in the final optimal Pareto front, respectively. The membership value ranges from 0 to 1, representing the satisfied degree of membership in a fuzzy set.

Secondly, obtain the final planning scheme according to the preference of decision maker. After determining the membership function to each objective function of every scheme, the decision maker needs to define the desirable level $\mu_{di}$ for each objective, and the final solution can be obtained by solving the following optimization problem:

$$\min_{X\in Solutionset}\ \sum_{i=1}^{m}\left|\mu_{di}-\mu_{fi}(x)\right|^2 \tag{54}$$

where the value of $\mu_{di}$ ranges from 0 to 1, and it reflects the degree of attention to the objective function $i$. For example, if we have enough investment budget and aim to minimize the production cost, the values of $\mu_{d1}$ and $\mu_{d2}$ can be set to 0 and 1 respectively.

## 4. Numerical results

### 4.1. Results analysis on the test system

The proposed model is tested on a combined energy system consisting of the IEEE 24-bus test system [28] and a 15-node natural gas network [6] to analyze the impact of wind power uncertainty on the CGEN expansion planning. These two networks are coupled via eight natural gas-fired generators as shown in Fig. 5. The natural gas network includes two sources, five gas loads (excluding the combined nodes), twelve gas pipelines and four compressors, where all compressors are treated as candidate infrastructures and node #1 serves as the reference node in the gas network. In addition, it is assumed that new pipelines can be added into each path of the gas network, and the maximum expansion number is two. The parameters of the candidate pipelines are the same as the existing ones on each path. The gas supply sources and gas demand will increase 1.5 times compared to the base year. The IEEE 24-bus system has thirty-eight existing lines, eight gas-fired generators and twenty-three coal-fired generators. Assuming that the system will be expanded for the future, the generation and load demand level equals to 2.2 times of their original values in the planning year. The candidate lines can be added into thirty-four existing corridors and seven new corridors 1–8, 2–8, 6–7, 13–14, 14–23, 16–23 and 19–23. Up to three candidate lines can be installed for these corridors. The carbon emission coefficient of gas-fired generator is assumed to be 0.549 ton/MW h and coal-fired generator 0.976 ton/MW h. The carbon price is $23/ton. The annualized investment cost for each gas compressor is $2 000 000.The annualized investment costs of electricity line and gas pipeline are $100 000/km and $150 000/km, respectively. All the detailed input data of the test system can be available from Appendices A and B.

The test is performed on a PC consisting of a 3.0-GHz processor and 2 GB of RAM. The proposed algorithm initializes the population size to be 80, and the probabilities of crossover and mutation to be 0.8 and 0.1, respectively.

To investigate the effects of the wind energy uncertainty on the integrated energy system, the generators on Bus-7, Bus-13 and Bus-23 are replaced by three wind farms A, B and C. The capacity of the three wind farms A, B, C is set to be 360 MW, 360 MW and 1000 MW, and the other generations are controlled by traditional thermal generators. The input data of wind farms are shown in Table 1. Furthermore, the effect of correlations among wind farms on the optimal Pareto front is studied on two cases: the correlation among wind farms is 0.8 in Case 2, while in Case 1 it is assumed that the outputs of the three wind farm are independent.

The results obtained by the proposed method are shown in Fig. 4, where it can be observed that the optimal Pareto front of case 1 is located in the front of Case 2. The reason is that the correlations among wind farms are positive and the variations of wind energy become stronger when the correlations are taken into consideration. Therefore, it will need more backup coal-fired or gas-fired generators and thus the total production cost increases in Case 2.

Furthermore, taking the Case 2 as an example, we consider four different desirable levels of two objectives by the fuzzy satisfying method on the optimal Pareto front. Tables 2 and 3 present the detailed expansion results of the natural gas network planning and electricity network planning. It should be noted that the desirable level is determined upon the attention level of the planner to the objective. In Table 4, total planning costs of the four schemes are presented. It can be seen that with the increase of the desirable level on investment cost, the investment cost is decreasing and the production cost is increasing, which reflects that the production cost of CGEN is closely related to the investment cost.

Moreover, the comparison of results of co-planning and separated planning (se-planning) of CGEN under the same desirable levels is shown in Tables 4 and 5, where it can be observed that the investment costs of se-planning is lower than that of co-planning, but the production cost is significantly higher. Loosely speaking, the total cost of co-planning is lower than that of se-planning. For all the four schemes, the total cost of co-planning is saved more than 10% than that of se-planning.

Choose the Scheme 3 for illustration, and the co-planning result is shown in Fig. 5. In the gas network, it can be observed that 12 new gas pipelines and two compressors are installed. Firstly, to

**Table 1**
Input data of wind farms.

| Wind farm bus | Scale parameter | Shape parameter | Vci (m/s) | Vrate (m/s) | Vco (m/s) |
|---|---|---|---|---|---|
| 7 | 5.90 | 1.51 | 3 | 12 | 25 |
| 13 | 5.93 | 2.03 | 3 | 12 | 25 |
| 23 | 5.12 | 1.99 | 3 | 12 | 25 |

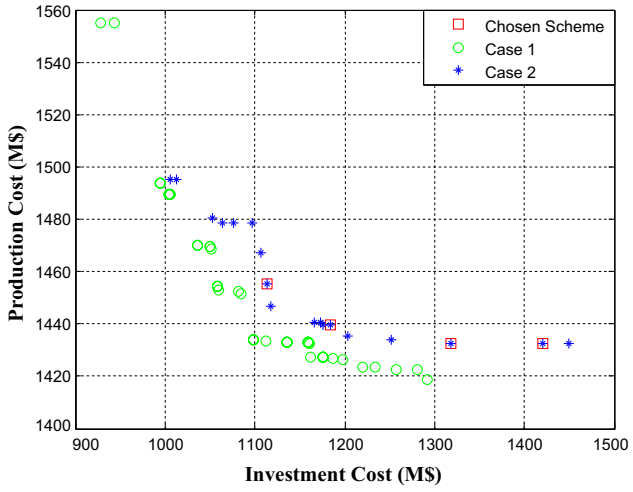


**Fig. 4.** Comparison of optimal Pareto fronts between Case1 and Case 2.

**Table 2**
Expansion results of the natural gas network on the four schemes.

| Candidate pipelines | | Scheme 1 | Scheme 2 | Scheme 3 | Scheme 4 |
|---|---|---|---|---|---|
| From node | To node | | | | |
| 1 | 3 | 2 | 2 | 2 | 2 |
| 2 | 4 | 2 | 2 | 1 | 2 |
| 3 | 4 | 0 | 0 | 0 | 0 |
| 3 | 5 | 2 | 2 | 2 | 1 |
| 4 | 7 | 1 | 1 | 2 | 1 |
| 6 | 9 | 2 | 2 | 2 | 0 |
| 8 | 11 | 2 | 2 | 1 | 2 |
| 10 | 13 | 2 | 2 | 1 | 2 |
| 12 | 14 | 2 | 2 | 1 | 2 |
| 13 | 14 | 0 | 0 | 0 | 0 |
| 13 | 15 | 1 | 1 | 0 | 0 |
| 14 | 15 | 1 | 1 | 0 | 1 |
| Candidate compressors | | Scheme 1 | Scheme 2 | Scheme 3 | Scheme 4 |
| Inlet node | Outlet node | | | | |
| 5 | 6 | 0 | 0 | 1 | 0 |
| 7 | 8 | 0 | 0 | 1 | 0 |
| 9 | 10 | 1 | 0 | 0 | 1 |
| 11 | 12 | 0 | 0 | 0 | 0 |

**Table 3**
Expansion results of the electricity network on the four schemes.

| Candidate electricity lines | | Scheme 1 | Scheme 2 | Scheme 3 | Scheme 4 |
|---|---|---|---|---|---|
| From bus | To bus | | | | |
| 1 | 2 | 0 | 0 | 0 | 0 |
| 1 | 3 | 0 | 0 | 1 | 0 |
| 1 | 5 | 3 | 1 | 0 | 1 |
| 1 | 8 | 0 | 0 | 0 | 0 |
| 2 | 4 | 0 | 0 | 0 | 0 |
| 2 | 6 | 0 | 0 | 0 | 0 |
| 2 | 8 | 0 | 0 | 0 | 0 |
| 3 | 9 | 1 | 1 | 0 | 0 |
| 3 | 24 | 1 | 1 | 1 | 1 |
| 4 | 9 | 0 | 0 | 2 | 0 |
| 5 | 10 | 0 | 0 | 0 | 0 |
| 6 | 7 | 0 | 0 | 0 | 0 |
| 6 | 10 | 3 | 3 | 1 | 3 |
| 7 | 8 | 2 | 2 | 1 | 1 |
| 8 | 9 | 0 | 0 | 0 | 0 |
| 8 | 10 | 1 | 1 | 1 | 1 |
| 9 | 11 | 1 | 1 | 1 | 1 |
| 9 | 12 | 1 | 1 | 0 | 1 |
| 10 | 11 | 1 | 1 | 0 | 1 |
| 10 | 12 | 0 | 0 | 1 | 0 |
| 11 | 13 | 0 | 0 | 1 | 0 |
| 11 | 14 | 0 | 0 | 2 | 0 |
| 12 | 13 | 0 | 0 | 1 | 0 |
| 12 | 23 | 0 | 0 | 0 | 0 |
| 13 | 14 | 0 | 0 | 0 | 0 |
| 13 | 23 | 1 | 1 | 0 | 1 |
| 14 | 16 | 1 | 1 | 2 | 1 |
| 14 | 23 | 0 | 0 | 0 | 0 |
| 15 | 16 | 0 | 0 | 0 | 0 |
| 15 | 21 | 0 | 0 | 0 | 0 |
| 15 | 24 | 1 | 1 | 0 | 0 |
| 16 | 17 | 1 | 1 | 2 | 1 |
| 16 | 19 | 2 | 0 | 0 | 2 |
| 16 | 23 | 0 | 0 | 0 | 0 |
| 17 | 18 | 0 | 0 | 1 | 0 |
| 17 | 22 | 0 | 0 | 0 | 0 |
| 18 | 21 | 0 | 0 | 1 | 0 |
| 19 | 20 | 0 | 0 | 0 | 0 |
| 19 | 23 | 0 | 0 | 0 | 0 |
| 20 | 23 | 1 | 1 | 0 | 1 |
| 21 | 22 | 0 | 0 | 0 | 0 |

ensure the natural gas to be sent out, all the gas pipelines connected gas suppliers and compressors are strengthened. Secondly, we can find that few gas pipelines connected to node #15 are expanded. The reason is that pressures at node #13 and #14 are improved by two compressors, respectively, so the pressure differences between #13-#15 and #14-#15 are capable of delivering enough natural gas to meet the gas demand $W_{L5}$. As for the electricity network, transmission lines are mostly added around the gas-fired generators. The reason is that both the production cost and carbon emission cost of gas-fired generators are lower than coal-fired generators, so as the capacity of electricity lines around gas-fired plants are improved, the cleaner power energy with lower price can be delivered as much as possible to meet the electricity demands. In addition, around the electricity nodes connected with wind farms (i.e., node #7, #13 and #23), lots of electricity lines are expected to be expanded because the total transmission capacity of the existing electricity lines is insufficient to ensure the wind energy, gas-fired generation and coal-fired generation to be fully sent out.

In contrast, Fig. 6 depicts the results of se-planning for the scheme 3. Unlike the planning results of gas network by co-planning, none of candidate compressors are selected by the se-planning, since the investment cost of compressor is relatively higher than gas pipelines. Thus, the inlet node and outlet node of each compressor becomes a same interconnection point. To ensure the gas to be delivered to each gas load, all the gas pipelines through the path from gas suppliers to the gas demand are expanded. As for the electricity network, transmission lines are only strengthened in the regional parts, such as bus #6, #8, #10 and #16, and the capacity expansion of electricity lines around gas-fired generators is not as strong as the planning results by co-planning.

The comparison between Figs. 5 and 6 shows that the co-planning can strengthen both electricity and gas network (i.e., installing two compressors) to improve the energy transfer capability to deliver more gas for balancing load demand, since the production cost of gas is relatively lower than coal. In contrast, the se-planning mainly strengthens the electricity network, and the production cost of electricity network and the total investment cost are reduced. However, the production cost of the gas network will be greatly increased, so that the total cost including both investment and production cost of CGEN is increased.

### *4.2. Results analysis on the real-life system*

In the future planning year, the predicted power energy of real-life electricity system of Hainan province (China) will be supplied by five types of units, including 8 gas-fired units (2986 MW), 17 coal-fired units (859 MW), 1 nuclear unit (650 MW), 10 hydro units (446 MW) and 3 wind farms (1080 MW). The wind speed data used here is data measured at the real power grid from January 1, 2014 to December 31, 2014 for every 15 min. The total peak load of planning horizon is 4364 MW. The electricity transmission network is mainly operated at two voltage levels, 110 kV and 220 kV, and there are 37 high-voltage substations and 431 existing transmission lines (including transformers). It is assumed that the candidate lines can be added into 27 existing corridors. Up to two candidate lines can be installed on each corridor. The natural gas network consists of two gas sources, eight gas loads (excluding the combined nodes), ten gas pipelines and three compressors, where all compressors are treated as candidate infrastructures and node #1 serves as the reference node in the gas network. In addition, candidate pipelines can be added into each path of the gas network, and the maximum expansion number is two. These two systems are coupled by A, B, C and D four natural gas power plants. The carbon emission coefficient, carbon price and

**Table 4**
Planning costs of schemes on different desirable levels.

| Name | Desirable level | | Co-planning | | Se-planning | |
|---|---|---|---|---|---|---|
| | | | Objective $f_1$ (M$) | Objective $f_2$ (M$) | Objective $f_1$ (M$) | Objective $f_2$ (M$) |
| Scheme 1 | 0.1 | 0.9 | 1420.122 | 1432.358 | 1344.194 | 1848.016 |
| Scheme 2 | 0.3 | 0.8 | 1318.050 | 1432.366 | 1231.177 | 1819.310 |
| Scheme 3 | 0.5 | 0.7 | 1183.724 | 1439.728 | 1102.722 | 1843.762 |
| Scheme 4 | 0.6 | 0.6 | 1113.592 | 1455.361 | 1063.295 | 1821.512 |

**Table 5**
Comparison of total planning cost on different desirable levels.

| Name | Co-planning total cost (M$) | Se-planning total cost (M$) | Percentage of total cost reduction (%) |
|---|---|---|---|
| Scheme 1 | 2852.480 | 3192.210 | 11.91 |
| Scheme 2 | 2750.416 | 3050.486 | 10.91 |
| Scheme 3 | 2623.453 | 3027.484 | 12.31 |
| Scheme 4 | 2568.953 | 2884.807 | 12.30 |

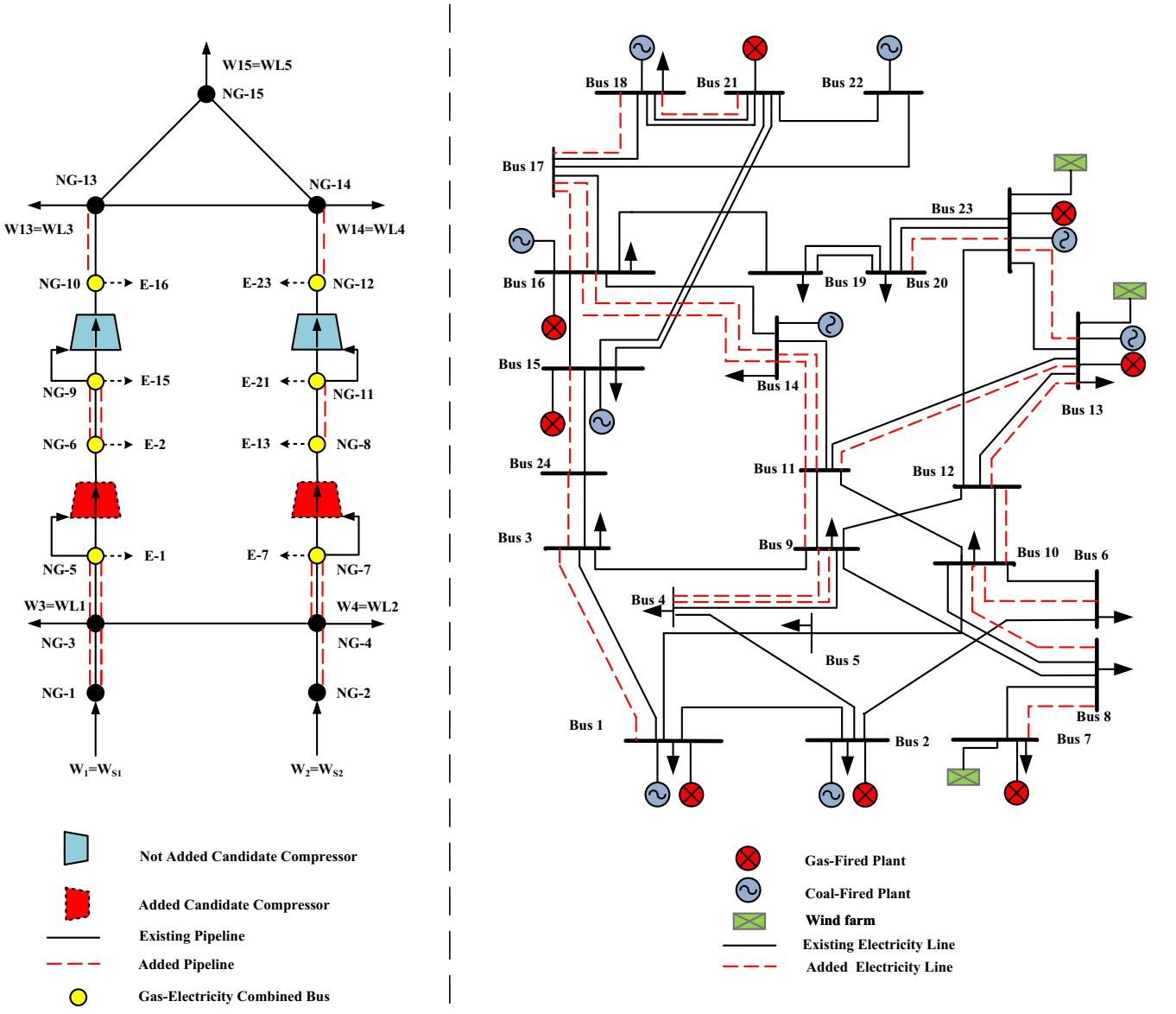


**Fig. 5.** Co-planning scheme (Scheme 3) of combined electricity and gas networks.

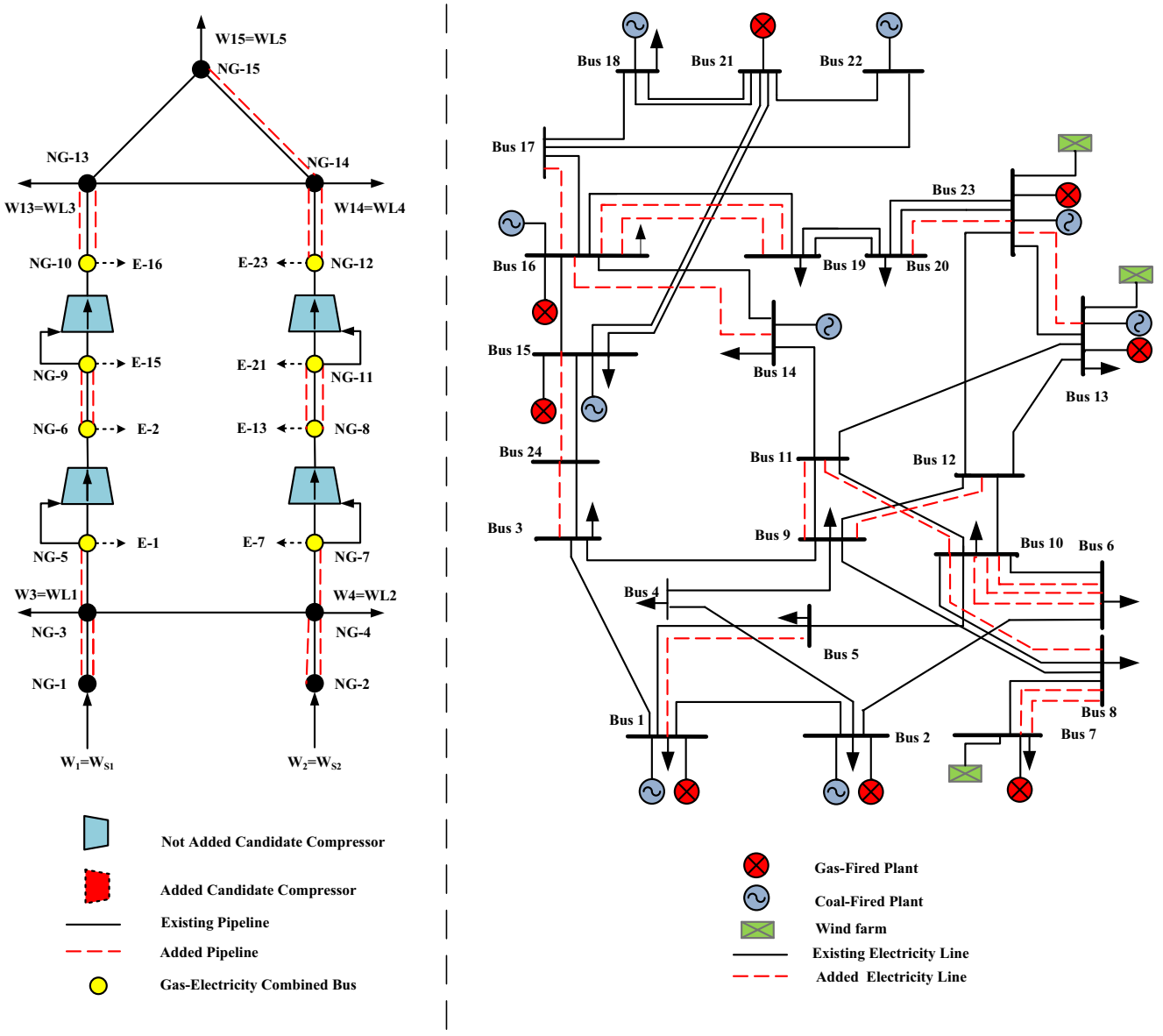


**Fig. 6.** Se-planning scheme (Scheme 3) of combined electricity and gas networks.

the annualized investment cost for each candidate elements are the same as the previous test system. All the data of this system comes from a National High Technology Research and Development Program of China (863 Program).

Fig. 7 depicts the optimal Pareto front of the planning result of the real-life system of Hainan province. Suppose that the budget of investment cost is enough and the aim of the planning project is to minimize the production cost. Thus, the desirable levels for investment cost and production cost can be chosen as 0.1 and 0.9, respectively. The final scheme marked in Fig. 7 will be chosen and the topology of the chosen co-planning result is shown in Fig. 8. Since Hainan province is an island and the middle of it is mountainous areas, the topology of the entire network is a ring structure with only three corridors connecting the East and West. It can be observed that most of the power plants are located in the west, especially for the gas-fired power plants. After adding new transmission lines on the base transmission network, transmission lines around wind farms and most gas-fired plants are strengthened to guarantee that cheaper and cleaner power energy can be sent out. The long distance transmission lines on corridor 1–34, 34–22

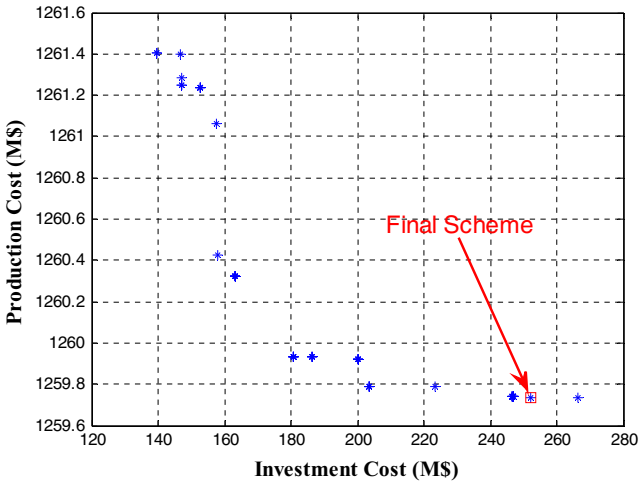


**Fig. 7.** Optimal Pareto front of real-life system.

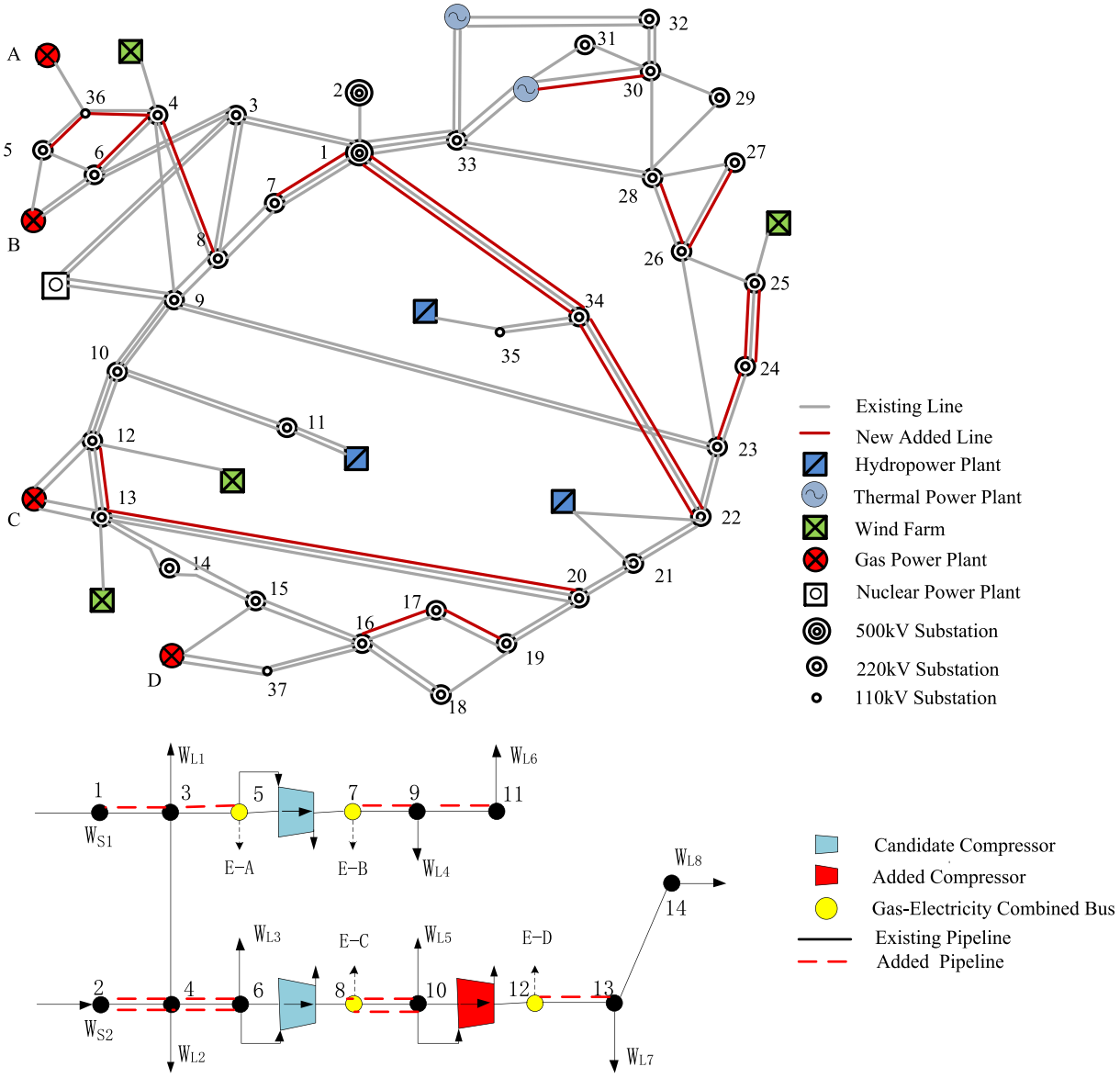


**Fig. 8.** Co-planning scheme of combined real-life electricity and gas system.

**Table 6**
Data of coal-fired generators.

| Node | Number | Capacity (MW) | Cost coefficient $a_i$ ($/MW$^2$) | Cost coefficient $b_i$ ($/MW) | Cost coefficient $c_i$ |
|---|---|---|---|---|---|
| 1 | 2 | 44 | 0.01131 | 12.145 | 0 |
| 1 | 1 | 167.2 | 0.01131 | 12.145 | 0 |
| 2 | 2 | 44 | 0.01131 | 12.145 | 0 |
| 2 | 1 | 167.2 | 0.01131 | 12.145 | 0 |
| 7 | 1 | 220 | 0.0122 | 17.924 | 0 |
| 13 | 1 | 433.4 | 0.003 | 20.023 | 0 |
| 14 | 2 | 44 | 0.01131 | 12.145 | 0 |
| 15 | 5 | 26.4 | 0.0667 | 9.2706 | 0 |
| 18 | 1 | 880 | 0.0028 | 5.345 | 0 |
| 22 | 6 | 110 | 0.001 | 0.5 | 0 |
| 23 | 1 | 880 | 0.00392 | 8.919 | 0 |

**Table 7**
Data of gas-fired generators.

| Node | Number | capacity (MW) | Gas fuel rate coefficient $\mu_1$ (BTU/MW$^2$) | Gas fuel rate coefficient $\mu_2$ (BTU/MW) | Gas fuel rate coefficient $\mu_3$(BTU) |
|---|---|---|---|---|---|
| 1 | 1 | 167.2 | 0.01131 | 12.145 | 0 |
| 2 | 1 | 167.2 | 0.01131 | 12.145 | 0 |
| 7 | 1 | 220 | 0.0122 | 17.924 | 0 |
| 13 | 1 | 833.4 | 0.003 | 20.023 | 0 |
| 15 | 1 | 341 | 0.0667 | 9.2706 | 0 |
| 16 | 1 | 341 | 0.0667 | 9.2706 | 0 |
| 21 | 1 | 880 | 0.0028 | 5.345 | 0 |
| 23 | 1 | 341 | 0.00392 | 8.919 | 0 |

and 13–20 are also newly added to enhance the original topology of electricity network. Although these lines have higher investment cost than other candidate lines, it can significantly reduce the production cost and improve the reliability of the whole system by strengthening the connection between the west and the east.

For the gas network, the transmission route between node #3 and node #11 is expanded by adding new pipelines, while on the transmission route between node #4 and node #14, not only the

**Table 8**
Data of load.

| Node | 1 | 2 | 3 | 4 | 5 | 6 | 7 | 8 | 9 | 10 | 13 | 14 | 15 | 16 | 18 | 19 | 20 |
|---|---|---|---|---|---|---|---|---|---|---|---|---|---|---|---|---|---|
| Load (MW) | 237 | 213 | 396 | 162 | 156 | 299 | 275 | 376 | 385 | 429 | 583 | 426 | 697 | 220 | 732 | 398 | 281 |

**Table 9**
Data of electricity lines.

| From bus | To bus | Reactance (p.u.) | Capacity (MW) | Number of existing lines | Max. number of expansion | Length (km) |
|---|---|---|---|---|---|---|
| 1 | 2 | 0.0139 | 175 | 1 | 3 | 3 |
| 1 | 3 | 0.2112 | 175 | 1 | 3 | 55 |
| 1 | 5 | 0.0845 | 175 | 1 | 3 | 22 |
| 1 | 8 | 0.1344 | 175 | 0 | 3 | 35 |
| 2 | 4 | 0.1267 | 175 | 1 | 3 | 33 |
| 2 | 6 | 0.192 | 175 | 1 | 3 | 50 |
| 2 | 8 | 0.1267 | 175 | 0 | 3 | 33 |
| 3 | 9 | 0.119 | 175 | 1 | 3 | 31 |
| 3 | 24 | 0.0839 | 400 | 1 | 3 | 50 |
| 4 | 9 | 0.1037 | 175 | 1 | 3 | 27 |
| 5 | 10 | 0.0883 | 175 | 1 | 3 | 23 |
| 6 | 7 | 0.192 | 175 | 0 | 3 | 50 |
| 6 | 10 | 0.0605 | 175 | 1 | 3 | 16 |
| 7 | 8 | 0.0614 | 175 | 1 | 3 | 16 |
| 8 | 9 | 0.1651 | 175 | 1 | 3 | 43 |
| 8 | 10 | 0.1651 | 175 | 1 | 3 | 43 |
| 9 | 11 | 0.0839 | 400 | 1 | 3 | 50 |
| 9 | 12 | 0.0839 | 400 | 1 | 3 | 50 |
| 10 | 11 | 0.0839 | 400 | 1 | 3 | 50 |
| 10 | 12 | 0.0839 | 400 | 1 | 3 | 50 |
| 11 | 13 | 0.0476 | 500 | 1 | 3 | 66 |
| 11 | 14 | 0.0418 | 500 | 1 | 3 | 58 |
| 12 | 13 | 0.0476 | 500 | 1 | 3 | 66 |
| 12 | 23 | 0.0966 | 500 | 1 | 3 | 134 |
| 13 | 14 | 0.0447 | 500 | 0 | 3 | 62 |
| 13 | 23 | 0.0865 | 500 | 1 | 3 | 120 |
| 14 | 16 | 0.0389 | 500 | 1 | 3 | 54 |
| 14 | 23 | 0.124 | 500 | 0 | 3 | 86 |
| 15 | 16 | 0.0173 | 500 | 1 | 3 | 24 |
| 15 | 21 | 0.049 | 500 | 2 | 3 | 68 |
| 15 | 24 | 0.0519 | 500 | 1 | 3 | 72 |
| 16 | 17 | 0.0259 | 500 | 1 | 3 | 36 |
| 16 | 19 | 0.0231 | 500 | 1 | 3 | 32 |
| 16 | 23 | 0.0822 | 500 | 0 | 3 | 114 |
| 17 | 18 | 0.0144 | 500 | 1 | 3 | 20 |
| 17 | 22 | 0.1053 | 500 | 1 | 3 | 146 |
| 18 | 21 | 0.0259 | 500 | 2 | 3 | 36 |
| 19 | 20 | 0.0396 | 500 | 2 | 3 | 55 |
| 19 | 23 | 0.0606 | 500 | 0 | 3 | 84 |
| 20 | 23 | 0.0216 | 500 | 2 | 3 | 30 |

**Table 10**
Bus data of gas network.

| Node | Supply capacity ($10^6$ SCF/h) | Load demand ($10^6$ SCF/h) | Minimum pressure (psia) | Maximum pressure (psia) |
|---|---|---|---|---|
| 1 | 20.288 | – | 600 | 1200 |
| 2 | 20.867 | – | 600 | 1200 |
| 3 | – | 1.838 | 500 | 1200 |
| 4 | – | 1.218 | 500 | 1200 |
| 5 | – | Gas-fired Plant | 400 | 1200 |
| 6 | – | Gas-fired Plant | 400 | 1200 |
| 7 | – | Gas-fired Plant | 400 | 1200 |
| 8 | – | Gas-fired Plant | 400 | 1200 |
| 9 | – | Gas-fired Plant | 400 | 1200 |
| 10 | – | Gas-fired Plant | 400 | 1200 |
| 11 | – | Gas-fired Plant | 400 | 1200 |
| 12 | – | Gas-fired Plant | 400 | 1200 |
| 13 | – | 4.263 | 600 | 1000 |
| 14 | – | 4.274 | 600 | 1000 |
| 15 | – | 1.501 | 600 | 1000 |

**Table 11**
Pipeline branch data of gas network.

| From node | To node | Pipeline constant | Number of existing lines | Max. number of expansion | Length (km) |
|---|---|---|---|---|---|
| 1 | 3 | 0.0320 | 1 | 3 | 80.5 |
| 2 | 4 | 0.0320 | 1 | 3 | 80.3 |
| 3 | 4 | 0.0128 | 1 | 3 | 55.9 |
| 3 | 5 | 0.0214 | 1 | 3 | 81.1 |
| 4 | 7 | 0.0103 | 1 | 3 | 87.9 |
| 6 | 9 | 0.0199 | 1 | 3 | 93.5 |
| 8 | 11 | 0.0125 | 1 | 3 | 99.7 |
| 10 | 13 | 0.0130 | 1 | 3 | 93.5 |
| 12 | 14 | 0.0060 | 1 | 3 | 97.9 |
| 13 | 14 | 0.0067 | 1 | 3 | 86.6 |
| 13 | 15 | 0.0070 | 1 | 3 | 79.7 |
| 14 | 15 | 0.0194 | 1 | 3 | 83.5 |

**Table 12**
Compressor branch data of gas network.

| Inlet node | Outlet node | Compressor constant | Gas consumption coefficient $\alpha$ | Gas consumption coefficient $\beta$ | Gas consumption coefficient $\gamma$ |
|---|---|---|---|---|---|
| 5 | 6 | 5420.58 | 0.0305 | 8.33 | 0 |
| 7 | 8 | 5356.05 | 0.0296 | 8.33 | 0 |
| 9 | 10 | 5420.58 | 0.0017 | 8.33 | 0 |
| 11 | 12 | 5356.05 | 0.0017 | 8.33 | 0 |

transmission capacity is increased, but also a new compressor is installed. The reason is that the transmission distance between node #4 and node #14 is longer than the distance between node #3 and node #11, so a compressor is needed to compensate the pressure loss along this route. It also can be found that after increasing the pressure at the node # 12 by the new added compressor, the natural gas can be sent to the terminate node #14 without investment for a new pipeline between #13 and #14.

## 5. Conclusions

A multi-objective CGEN co-planning model is developed to search for the optimal scheme of the combined natural gas and electricity network to coordinate different objectives, which can effectively handle the expansion planning problem about *which* and *where* natural gas pipes, gas compressors and power transmission lines are expanded in the integrated natural gas network and electricity network. Moreover, the impact of the uncertainties and correlations of the wind farms on the total production cost is revealed that the stochastic wind power may increase the total cost of CGEN. Most importantly, the proposed model is performed on a test system and a real-life system, which achieves a higher social welfare than the design with each separated networks.

Technically, the proposed multi-objective optimization model is solved by the Elitist Non-dominated Sorting Genetic Algorithm II (NSGA-II) to capture the optimal Pareto front. Therein, the combined optimal power and natural gas load flow, served as a subproblem of the original multi-objective optimization model, is tackled by the proposed primal–dual interior-point method combined with the improved point-estimation method. This method is actually a general approach that also can be extended to other research fields with the consideration of different kinds of uncertainties, such as natural gas price, natural gas load and electricity load.

## Appendix A. Data of test electricity system

Tables 6–9.

## Appendix B. Data of natural gas test system

Tables 10–12.

## References


[1] Üster H, Dilaveroğlu Ş. Optimization for design and operation of natural gas transmission networks. Appl Energy 2014;133:56–69.
[2] Ozturk M, Yuksel YE, Ozek N. A bridge between east and west: Turkey's natural gas policy. Renew Sustain Energy Rev 2011;15(9):4286–94.
[3] International energy agency. World energy, Outlook 2010; 2010.
[4] De Gouw JA, Parrish DD, Frost GJ, Trainer M. Reduced emissions of CO2, NOx, and SO2 from US power plants owing to switch from coal to natural gas with combined cycle technology. Earth's Future 2014;2(2):75–82.
[5] Chaudry M, Jenkins N, Qadrdan M, Wu J. Combined gas and electricity network expansion planning. Appl Energy 2014;113:1171–87.
[6] An S, Li Q, Gedra TW. Natural gas and electricity optimal power flow, transmission and distribution conference and exposition. IEEE Power Eng Soc 2003;1:138–43.
[7] Martínez-Mares A, Fuerte-Esquivel CR. A unified gas and power flow analysis in natural gas and electricity coupled networks. IEEE Trans Power Syst 2012;27(4):2156–66.
[8] Chaudry M, Jenkins N, Strbac G. Multi-time period combined gas and electricity network optimisation. Electr Power Syst Res 2008;78(7):1265–79.
[9] Correa-Posada CM, Sánchez-Martın P. Security-constrained optimal power and natural-gas flow. IEEE Trans Power Syst 2014;29(4):1780–7.
[10] Liu C, Shahidehpour M, Wang J. Coordinated scheduling of electricity and natural gas infrastructures with a transient model for natural gas flow. Chaos: An Interdiscipl J Nonlinear Sci 2011;21(2):025102.
[11] Liu C, Shahidehpour M, Fu Y, Li Z. Security-constrained unit commitment with natural gas transmission constraints. IEEE Trans Power Syst 2009;24(3):1523–36.
[12] Liu C, Shahidehpour M, Wang J. Application of augmented Lagrangian relaxation to coordinated scheduling of interdependent hydrothermal power and natural gas systems. Gener Transm Distrib 2010;4(12):1314–25.
[13] Unsihuay-Vila C, Marangon-Lima JW, Perez-Arriaga IJ, Balestrassi PP. A model to long-term, multiarea, multistage, and integrated expansion planning of electricity and natural gas systems. IEEE Trans Power Syst 2010;25(2):1154–68.
[14] Barati F, Seifi H, Sepasian MS, Nateghi A, Shafie-khah M, Catalão JP. Multi-period integrated framework of generation, transmission, and natural gas grid expansion planning for large-scale systems. IEEE Trans Power Syst 2014 [online].
[15] Qiu J, Dong ZY, Zhao JH, Meng K, Zheng Y, Hill DJ. Low carbon oriented expansion planning of integrated gas and power systems. IEEE Trans Power Syst 2015;30(2):1035–46.
[16] Chompoo-Inwai C, Lee W, Fuangfoo P, Williams M, Liao J. System impact study for the interconnection of wind generation and utility system. Ind Appl 2005;41(1):163–8.
[17] Cui X, Li W, Ren X, Xue F, Fang Y. Review of transmission planning with large-scale wind power integration. 2012 Electromagn Comp (APEMC) 2012:285–8.
[18] Qadrdan M, Chaudry M, Wu J, Jenkins N, Ekanayake J. Impact of a large penetration of wind generation on the GB gas network. Energy Policy 2010;38(10):5684–95.
[19] Martinez-Mares A, Fuerte-Esquivel CR. A robust optimization approach for the interdependency analysis of integrated energy systems considering wind power uncertainty. IEEE Trans Power Syst 2013;28(4):3964–76.
[20] NERC. NERC planning standard; 1997.
[21] Wei H, Li F, Zijun H, Junzhao C, Li Z. Transmission network planning with N-1 security criterion based on improved multi-objective genetic algorithm. Electr Utility Deregul Restruct Power Technol (DRPT) 2011:1250–4.
[22] Deb K, Pratap A, Agarwal S, Meyarivan T. A fast and elitist multiobjective genetic algorithm: NSGA-II. Evol Comput 2002;6(2):182–97.
[23] Hedman KW, O'Neill RP, Fisher EB, Oren SS. Optimal transmission switching with contingency analysis. IEEE Trans Power Syst 2009;24(3):1577–86.
[24] Morales JM, Baringo L, Conejo AJ, Mínguez R. Probabilistic power flow with correlated wind sources. Gener Transm Distrib 2010;4(5):641–51.
[25] Justus CG, Hargraves WR, Yalcin A. Nationwide assessment of potential output from wind-powered generators. J Appl Meteorol 1976;15(7):673–8.
[26] Wang X, Gong Y, Jiang C. Regional carbon emission management based on probabilistic power flow with correlated stochastic variables. IEEE Trans Power Syst 2015;30(2):1094–103.
[27] Moeini-Aghtaie M, Abbaspour A, Fotuhi-Firuzabad M. Incorporating large-scale distant wind farms in probabilistic transmission expansion planning—Part I: Theory and algorithm. IEEE Trans Power Syst 2012;27(3):1585–93.
[28] Fang R, Hill DJ. A new strategy for transmission expansion in competitive electricity markets. IEEE Trans Power Syst 2003;18(1):374–80.